Alfvén's Critical Velocity Effect Tested in Space

Gerhard Haerendel

Max-Planck-Institut für Physik und Astrophysik, Institut für extraterrestrische Physik, Garching bei München

Z. Naturforsch. **37a**, 728–735 (1982); received July 6, 1982

To Professor Arnulf Schlüter on his 60th Birthday

A sounding rocket experiment involving the injection of a barium gas jet in the upper ionosphere provided an opportunity of investigating quantitatively several aspects of the beam-plasma interaction that is the substance of Alfvén's critical velocity effect. Whereas the experimental data are presented elsewhere, this paper contains some theoretical considerations of (1) the limiting neutral density for which the ionization process can operate, (2) the interaction of the freshly injected ions with the background plasma, and (3) the microprocess which leads to collisionless electron tail formation. The observed distribution of injected ions is consistent with the Townsend condition on the beam-plasma discharge. The mass loading on the ambient plasma, although locally high, has a weak effect on the dynamics of the involved flux-tube because of the limited extent of the beam. The most likely process by which energy is transferred from the freshly generated ions to the electrons is an ion beam instability leading to the excitation of lower hybrid waves.

Introduction

Alfvén's [1] critical velocity effect is an efficient ionization process that can act on a beam of neutral particles crossing a magnetized plasma. Their relative velocity in the direction transverse to the magnetic field, $v_{n\perp}^*$, must exceed a limiting value which depends on the ionization potential, V_{ion}, of the neutrals:

$$v_{n\perp}^* > v_{crit} = \sqrt{\frac{2\,e\,V_{ion}}{m_n}} \qquad (1)$$

(m_n is the mass of the neutral particle).

The process is essentially a beam plasma discharge, whereby the energy is drawn from the transverse kinetic energy of the neutrals in the plasma frame. An instability of the freshly generated ions leads to wave excitation and resonant heating of the electrons up to and above the ionization threshold. The discharge can burn if the tail electrons make at least one ionizing collision during the time of contact, τ_{inj}, with the neutral beam (Townsend condition). This implies a lower limit on the neutral density. An upper limit arises from the collisionless nature of the ion-electron interaction.

The critical velocity effect was proposed by Alfvén [1] in a theory of planetary formation where it provided a means of separation of elements depending on their ionization potential. The effect has been studied extensively in the laboratory [2–7]. After the work of Sherman [8] theoretical investigations [5, 9, 10] focussed on some kind of lower hybrid drift instability as the means of coupling the kinetic energy of the injected ions to the electrons. Besides the protoplanetary nebula, many other astrophysical situations have been thought to be sites of this effect [11], e. g. cometary comae [12, 13] and the atmospheres of non- magnetized planets [14], such as Venus, as they interact with the solar wind, and the atmospheres of satellites like Io [15] in rotating planetary magnetospheres. Space experiments with neutral gas injection of elements with v_{crit} below the orbital velocity of the spacecraft have also been proposed [16].

Another means of achieving relative velocities of a neutral gas and a natural plasma well above v_{crit} is the *shaped charge technique* [17]. The hollow cone of the high explosive is covered with a metal liner. Upon explosion gas jets with speeds exceeding 10 km/s are created. This technique has been employed frequently in order to inject barium ion jets, which result readily from photo-ionization, into the lower magnetosphere for probing of the electric field [18, 19].

This report deals with the experimental situation in which such a neutral gas jet interacts with the plasma of the upper ionosphere where the densities are sufficiently low for collisionless ion-electron

Reprint requests to Dr. G. Haerendel, Max-Planck-Institut für Physik und Astrophysik, Institut für extraterrestrische Physik, Gießenbachstr., D-8046 Garching bei München.

0340-4811 / 82 / 0800-0728 $ 01.30/0. — Please order a reprint rather than making your own copy.

interactions. A sounding rocket flight of a complex payload with plasma diagnostic instruments and, among others, a separable shaped charge provided an occasion of studying this effect in great detail [11]. The data are discussed in a separate paper which will be referred to as Paper 2. A similar experiment was performed by Deehr et al. (1982) [20] using barium and strontium, but without any in-situ diagnostics. After a brief presentation of the experimental situation and the observations, we will deal with essentially three subjects, the limits on the neutral gas density for the existence of the critical velocity effect, the momentum coupling to the ambient plasma, and the nature of the microprocess achieving the energy transfer to the electrons.

The Experiment

A barium gas exposed to sunlight is photo-ionized with a time constant of 20 – 30 sec. This is the basis of experimenting with barium plasma clouds and jets in ionosphere and magnetosphere [19]. For a critical velocity experiment, one wants to suppress the rapid photo-ionization process, but needs sunlight for the optical diagnostics. An obvious solution is to inject the gas jet inside the earth's shadow, not much below the terminator, and orient the jet's axis so that the generated ions travel quickly along the magnetic lines of force upward into sunlight. Figure 1 illustrates the situations during the third flight of Project Porcupine in ESRANGE/Kiruna on March 19, 1979. The angle between the jet axis and $\boldsymbol{B}$ was 28°. This way a large fraction of the atoms had transverse velocity components exceeding the critical velocity of 2.7 km/s. A typical velocity distribution for such charges [21] is shown in Figure 2. Any ions created initially near the point of explosion should appear in form of a narrow streak on the western edge of the ion cloud when reaching sunlight. The eastern flank should have a rather diffuse profile constituted by the ions formed out of the remaining neutral atoms when passing the terminator. Width and inclination of the jet were such that the con-

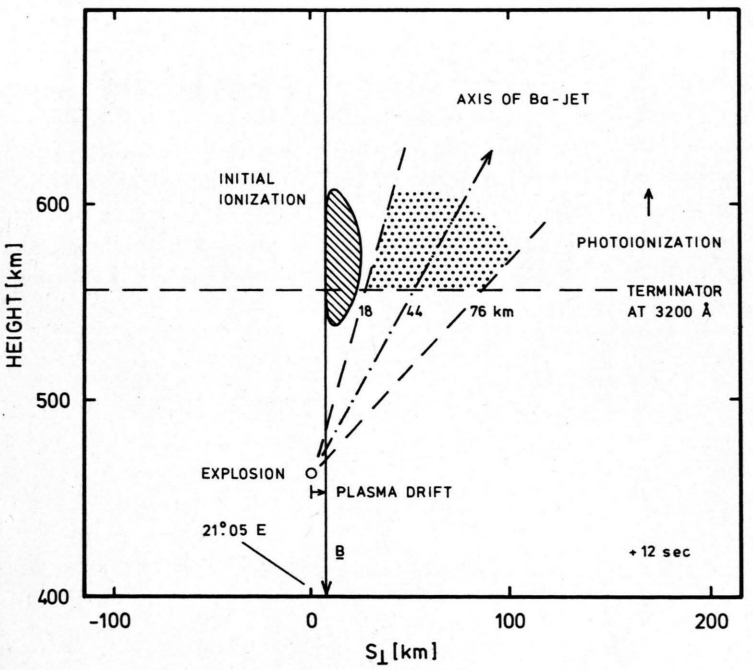

Fig. 1. Geometry of the Ba gas jet injected from the Porcupine rocket above ESRANGE on March 19, 1979. The shaped charge was ignited about 100 km below the terminator with the axis inclined towards the east by 28°.

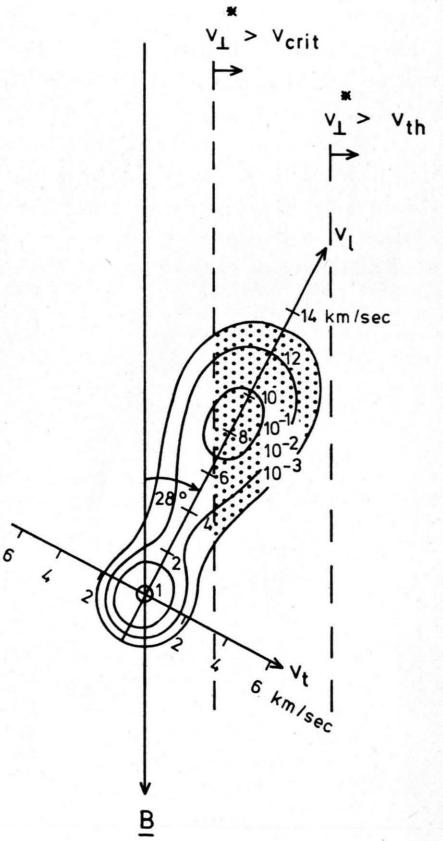

Fig. 2. Typical velocity distribution of a shaped charge generated Ba-jet after Koons and Pongratz [21]. The dotted part exceeds v_{crit} in the plasma frame.

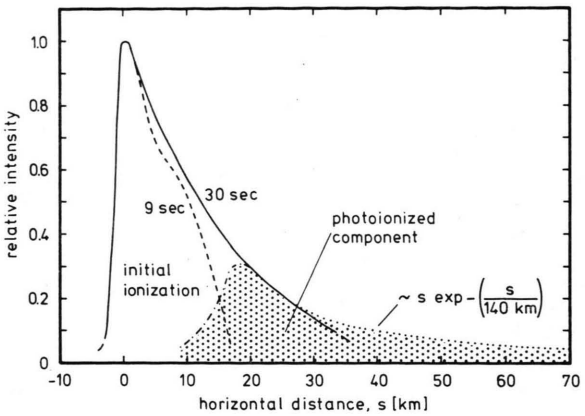

Fig. 3. Densitometer traces of the ionized barium cloud appearing above the terminator. The dotted part is a fit of the data to the expected contribution from photo-ionization. Nearly all ions to the left of $s = 15$ km are the result of an initial ionization in darkness.

tribution of photo-ionization to the Ba ions found between the field line of injection and one 15 km to the east was minimal. Figure 3 shows two densitometer traces through the ion cloud in west-east direction. The initially created ions are concentrated within 15 km from the field line of explosion and represent about 30% of the atoms with $v_{n\perp}^{*} > v_{crit}$ (cf. Figure 2).

Obviously, there are two interpretations of the initial ionization. It might have been generated within very short distance from the point of explosion, and the ions may have been re-distributed over a transverse range of ≈ 15 km owing to their high initial momentum, or they were injected essentially at the field line along which they appear in sunlight. Considerations of the momentum coupling supported by measurements of the electric field outside the beam exclude the first hypothesis, as will be demonstrated below. In particular, the contribution of thermal ionization in the explosion phase cannot have been significant, quite in agreement with other experimental evidence and theory. They pose an upper limit of 1% (see Paper 2). The only remaining possibility is that of collisional ionization. This implies a number density of electrons above 5.2 eV ($= eV_{ion}(\mathrm{Ba})$) exceeding even the most intense auroral electron fluxes by 5 to 6 orders of magnitude. No other explanation than a beam-plasma discharge appears to be possible.

The relatively fast cut-off of the initial ionization at a transverse range of about 15 km must be interpreted as the result of the neutral density falling below the lower threshold for the critical velocity effect. It was near $3 \cdot 10^5\ \mathrm{cm}^{-3}$ when averaged over the fast part of the gas jet. Along the axis it might have been higher by a substantial factor. Unfortunately, we have no high resolution data of the velocity profile.

The configuration of the Ba-charge with respect to the diagnostic payloads (main payload and two separable subpayloads) was such that no direct contact between gas jet and diagnostic instruments was achieved. This is shown in Figure 4. Hence neither the electrostatic turbulence which leads to electron heating nor the suprathermal electrons could be

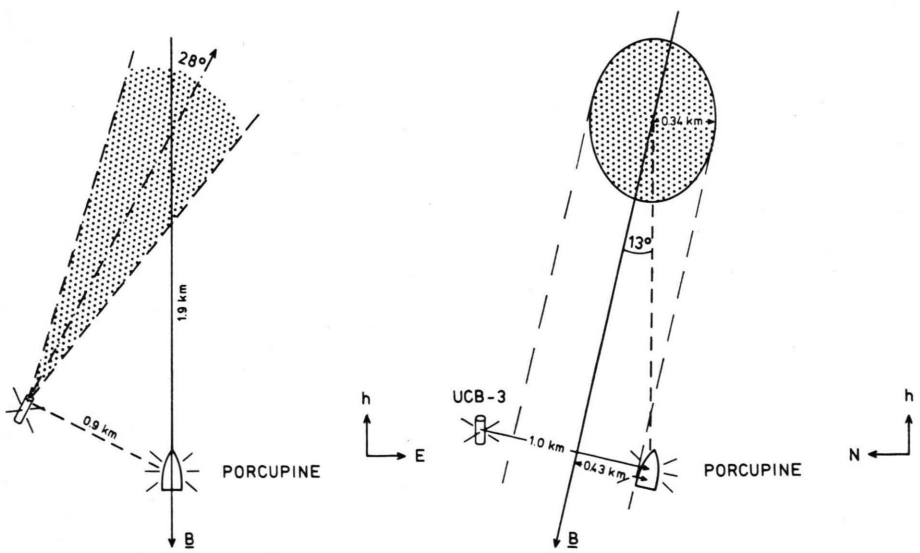

Fig. 4. Geometry of barium jet and Porcupine payload in two perpendicular vertical planes. UCB-3 is the closest of the instrumented subpayloads.

measured at their peak intensity. Only several orders of magnitude reduced fringe effects were observed. This is not so with regard to the d.c. electromagnetic field. All six components ($\boldsymbol{B}$ and $\boldsymbol{E}$) exhibited significant perturbations in the range of $(10-30)$ nT and $(6-20)$ mV/m. Their interpretation is given in terms of the diamagnetic effect of the injected plasma ($\Delta B_{\parallel}$), the electric polarization field restraining the hot electrons along the field lines ($E_{\parallel}$), and the excitation of shear Alfvén-waves ($\Delta \boldsymbol{B}_{\perp}, \Delta \boldsymbol{E}_{\perp}$) (cf. Paper 2). Indeed, the observed ratios of the corresponding components of $\Delta \boldsymbol{E}_{\perp}$ and $\Delta \boldsymbol{B}_{\perp}$ agree well with the local Alfvén velocity.

Subsequently, we will deal with the three most interesting aspects of the experiment, the neutral density limits, the momentum transfer to the background plasma and the nature of the basic instability.

Neutral Density Limits

A crucial aspect of any discharge is the energy balance. It must be positive, i. e. the energy gained between two ionizing collisions must exceed the ionization energy. In the present context, the energy is liberated simultaneously with the ionization process, but it resides at first in the ions and must be transferred to the electrons. Part of the energy ($\frac{1}{2} m_n v_{n\perp}^{*2}$) will be converted into thermal energy of the ions, only a fraction η_e is available for electron heating. The electrons are divided into bulk electrons with density n_e and mean energy gain ΔW_e, and tail electrons (n_T) with energy gain ΔW_T. We can put the separation line between the two components arbitrarily at the ionization threshold ($\Delta W_T > e V_{ion}$). If heat losses of the electrons are designated by L, we can write their energy balance as

$$\{\eta_e \tfrac{1}{2} m_n v_{n\perp}^{*2} - e V_{ion}\} \dot{n}_i \tau_{inj} = \Delta W_T n_T + \Delta W_e n_e + L . \quad (2)$$

The ionization rate, $\dot{n}_i$, is defined as

$$\dot{n}_i = n_n n_T \langle \sigma_{ion} v_T \rangle , \quad (3)$$

where σ_{ion} is the energy dependent ionization cross-section and v_T the average speed of the tail electrons. More accurately we must replace $\dot{n}_i \tau_{inj}$ by an integral. We determine $\langle \sigma_{ion} v_T \rangle$ at 10 eV where the cross-section has the maximum value of $1.2 \cdot 10^{-15}$ cm^2 [22]. The injection time, τ_{inj}, is the passage time of the neutral beam through a given plasma element. Neglecting the losses, L, and replacing $\Delta W_T / e V_{ion}$ by unity we find a lower limit on the neutral density from the foregoing equations,

$$n_n > \frac{1 + \dfrac{\Delta W_e}{e V_{ion}} \cdot \dfrac{n_e}{n_T}}{\left\{ \eta_e \left(\dfrac{v_{n\perp}^*}{v_{crit}} \right)^2 - 1 \right\} \langle \sigma_{ion} v_T \rangle \tau_{inj}} . \quad (4)$$

Evaluation of the brightness profile of the ions (see Figure 3) provides information on the development of n_T along the expanding neutral beam. n_T grows with time and reaches a maximum close to the value of the ambient density shortly before the process dies out at a range of 15 km. This shows that our subsequent neglect of the second term in the numerator does not necessarily lower the density limit in an unrealistic fashion.

Introducing the frequency of ionizing collisions for the tail electrons

$$\nu_{ion} = n_n \langle \sigma_{ion} v_T \rangle , \quad (5)$$

we can write the lower density limit in the simple fashion

$$\nu_{ion} \tau_{inj} > \left\{ \eta_e \left(\frac{v_{n\perp}^*}{v_{crit}} \right)^2 - 1 \right\}^{-1} . \quad (6)$$

Equations (4) and (6) show that the true threshold velocity is not v_{crit} but $\eta_e^{-1/2} v_{crit}$. The value of η_e is crucial. For our experiment with $\langle v_{n\perp}^{*2} \rangle$ being only about $4 v_{crit}^2$, η_e must have been $\gtrsim 0.5$. Otherwise the ionization process should have been very inefficient. Such a value is, however, quite consistent with theoretical considerations [9, 10], computer simulations [23] and the implications of some laboratory experiments [7] yielding between 28 and 67%. The latter value was derived for the instability of a linear ion beam [10].

Replacing the r.h.s. of (6) by unity,

$$\nu_{ion} \tau_{inj} > 1 , \quad (7)$$

means that a tail electron makes at least one ionizing collision during the time of contact with the beam [24]. This is the minimum needed for maintenance of the discharge. We can call it the Townsend condition. Even if $v_{n\perp}^*$ were so high as to lower the r.h.s. of (6) much below unity, this would not constitute a realistic lower limit; (7) would still apply.

The limiting neutral density would thus be

$$n_n \gtrsim (\langle \sigma_{ion} v_T \rangle \tau_{inj})^{-1} , \quad (8)$$

which for our experiment turns out to be $9 \cdot 10^5\,\mathrm{cm}^{-3}$, or a factor of 3 higher than deduced from the transverse range of initial ionization. The discrepancy is likely to result from a somewhat stronger concentration of the beam density towards the axis than assumed in the earlier estimates.

Finally, there is also an upper limit to the neutral density. It is derived from the condition of a collisionfree plasma on time-scales of the order of the growth-rate, γ, of the beam instability [4, 25]. With ν_{en} being the electron-neutral collision frequency and $\gamma \approx \frac{1}{2}\Omega_{LH}$ [23], we can find an upper density limit from:

$$\nu_{en} \lessapprox \tfrac{1}{2}\Omega_{LH}\,, \tag{9}$$

Ω_{LH} being the lower hybrid frequency. For our experiment it implies that the discharge started to build up beyond about 200 m from the field line of beam injection.

The considerations of this section show that the neutral density of the barium vapor jet was sufficiently high for a beam-plasma discharge to develop inside a range of ≈ 15 km from the point of origin. However, the resulting ionization is difficult to predict. Only after having considered the momentum exchange with the background plasma will it be possible to conclude that the injected ions must have been produced on the field lines along which they appeared above the terminator. A more concentrated production and later re-distribution can then be ruled out. This means that the discharge actually burnt until n_n reached approximately the limit predicted by (8).

Momentum Transfer

Ionization by the critical velocity process is analogous to the inelastic collision of two masses, one being the newly created ions, the other the background plasma. If the former exceeds the latter substantially, most of the energy will be retained by the conservation of momentum and little will be left for inelastic processes. In the opposite case, there is little limitation on the fraction of energy consumed. The barium injection in our experiment created a strong enhancement of the mass density of the plasma. However, contrary to laboratory set-ups, the interaction volume of beam and plasma cannot be considered in isolation. Momentum can be taken up by the magnetic field and carried away by shear Alfvén waves. Thus, in a low β plasma a much larger volume participates in the momentum balance. This is sketched in Figure 5.

In order to establish the relation between the two colliding masses, we must compare the mass injected into a flux-tube of cross-section A,

$$m_n \dot{n}_i\, l_{||}\, A$$

(where $l_{||}$ is the diameter of the beam $\| \boldsymbol{B}$) with the mass covered per unit time by the two Alfvén waves emitted in either direction along the field lines,

$$2\,\varrho_a\, v_A\, 2\,A\,,$$

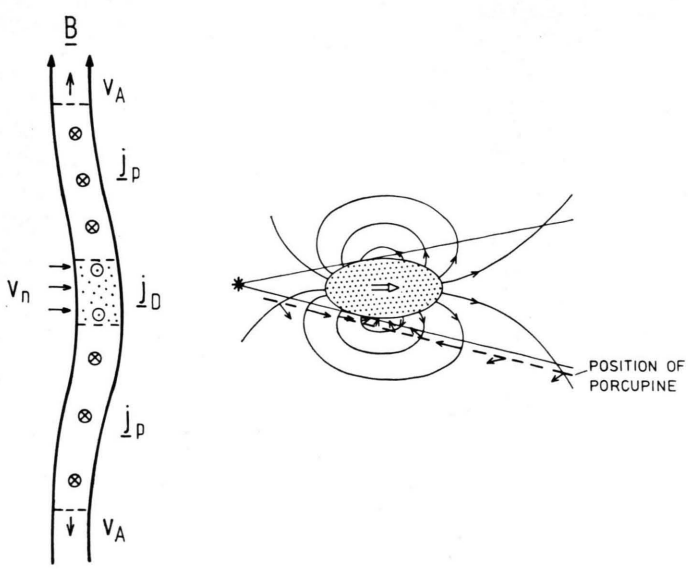

Fig. 5. (left) Bending of the magnetic lines of force caused by the mass injection. The dynamo current, j_D, at the level of injection connects via field-aligned currents with the polarization current, j_p, in the plasma background. (right) Horizontal cut through the injection region showing the plasma circulation initiated by the injected plasma. — Arrows along the dashed line represent the electric field at the position of the Porcupine payload.

v_A being the Alfvén velocity. The second factor of 2 takes care of the fact that the affected volume in an incompressible medium is effectively twice the volume of injection. This is sketched on the r.h.s. of Figure 5. We call the ratio of the above quantities,

$$\lambda_M = \frac{m_n \dot{n}_i l_{||}}{4 \varrho_a v_A}, \tag{10}$$

the *mass loading factor*. $\lambda_M = 1$ corresponds to the case of two equal masses colliding with each other.

The observed ion distribution can be interpreted in terms of $\dot{n}_i (= n_i/\tau_{inj})$. It implies that beyond about 350 m from the point of injection $(\perp \boldsymbol{B})\lambda_M$ fell below unity. Hence, for most of the injection we had the case of weak mass loading.

The upper limit on the kinetic energy that can be expended in an inelastic collision of two point masses is given by $(1+m_1/m_2)^{-1}$. If we replace m_1/m_2 by λ_M we should get a reasonable limit for the fraction, η_e, of the energy $\frac{1}{2} m_n v_{n\perp}^{*2}$ transferred to the electrons:

$$\eta_e \lesssim (1+\lambda_M)^{-1}. \tag{11}$$

As $\lambda_M < 1$ for most of the interaction, we can conclude that η_e was not severely restricted by the momentum balance but rather by the nature of the instability. $\eta_e \gtrsim 0.5$ as derived above is entirely possible.

The fraction, α_m, of the momentum corresponding to the energy transferred to the electrons is carried away by the two Alfvén waves. The amplitude of the waves is determined by the balance of Lorentz force and momentum injection,

$$B j_D = \alpha_m m_n v_{n\perp}^* \dot{n}_i. \tag{12}$$

j_D is the dynamo current in the circuit established along the flux-tube of mass injection (see Figure 5). The current closure is provided by polarization currents, j_p, in the background plasma with density ϱ,

$$j_p = \frac{\varrho}{B^2} \frac{\partial E_\perp}{\partial t} \tag{13}$$

$$\left(\left| \frac{1}{E_\perp} \frac{\partial E_\perp}{\partial t} \right| \ll \Omega_i(O^+) \right).$$

The current balance

$$j_D l_{||} = j_p 4 v_A \tau_{inj} \tag{14}$$

combined with the preceding equations yields

$$\frac{\partial E_\perp}{\partial t} = \lambda_M \frac{\alpha_m E_\perp^*}{\tau_{inj}} \tag{15}$$

with

$$E_\perp^* = v_{n\perp}^* B. \tag{16}$$

Of course, $E_\perp$ is not constant along the flux-tube. It must be considered as a characteristic value. When $\lambda_M \ll 1$, $E_\perp$ will build up to a maximum at the end of the injection phase of the order of

$$\Delta E_\perp \approx (\partial E_\perp/\partial t)\tau_{inj} = \lambda_M \alpha_m E_\perp^*. \tag{17}$$

This equation gives us a handle on the interpretation of the observed electric perturbation field. $\Delta E_\perp$ must be substantially smaller than the field $E_\perp^*$ corresponding to the neutral particle velocity. The maximum of $\Delta E_\perp$ was $0.2 E_\perp^*$. As λ_M is estimated to be ≈ 0.4 at the distance of the Porcupine payload, we can derive a value of $\alpha_m \approx 0.5$. This would be in agreement with our previous conclusion that $\eta_e \gtrsim 0.5$. However, the present determination must be regarded as rather uncertain.

In case of high mass loading, $E_\perp$ would grow rapidly towards $E_\perp^* - v_{crit} B$ and stabilize somewhat below. This means that the plasma would lag the neutrals by a value close to, but above the critical velocity. This is typically observed in the laboratory experiments. The stabilization is easily achieved by an adjustment of the mass injection rate which in turn determines λ_M. The advantage of low mass loading for the efficiency of the effect lies in the fact that the free energy, $\frac{1}{2} m_n v_{n\perp}^{*2}$, is not reduced by acceleration of the plasma frame.

At the end of the injection phase, $E_\perp$ starts to decay with the time constant [26]

$$\tau_0 = \lambda_M \tau_{inj}. \tag{18}$$

Now we are in the position to substantiate our earlier argument that the spatial extent of the observed ionization is indicative of the actual range of operation of the critical velocity effect. Converting the ion density into $\dot{n}_i$ and λ_M shows that already at one half of the observed extent (7.5 km), $\lambda_M \approx 0.03$. Thus, even if initially $\lambda_M \gg 1$, a re-distribution over such a range would not have been consistent with the rapid momentum loss.

Microprocesses

The heart of the critical velocity process is the transfer of energy from the newly created ions to the electrons. Both theoretical and experimental work have narrowed down the process to some kind of modified two-stream instability. The dominant frequency excited is the lower hybrid frequency,

Ω_{LH}. It is satisfactory that the electric wave detector as well as the Langmuir probe measuring density fluctuations on the Porcupine payload showed a sudden increase of noise below 2 kHz ($\triangleq \Omega_{LH}/2\pi$) at Ba injection. However, being recorded far outside the interaction volume, the signals were much below the level needed for electron heating.

With regard to the detailed mechanism, two different cases have been discussed, an instability of the beam of injected ions [8–10] and an instability of the electric current driven by a polarization field E_p which arises from charge separation in the ionization front [5]. The two mechanisms are sketched in Figure 6. The first one can be further subdivided according to the magnitude of the ionization rate, $\dot{n}_i$ [10]. If the beam density is comparable to that of the background, the growth-rate of the instability is of the order of Ω_{LH}, i. e. $\gg \Omega_i$. Hence the gyromotion of the ions is entirely negligible; they form a linear beam. For this case, Galeev [10] derived $\eta_e = 2/3$. With decreasing ionization rate the growth-rate approaches Ω_i. This should occur when

$$\frac{\dot{n}_i}{n_i} \approx \sqrt{\frac{m_e}{m_i}}\,\Omega_i\,, \tag{19}$$

or

$$\Omega_i\,\tau_{inj} \approx \sqrt{\frac{m_i}{m_e}}\,. \tag{20}$$

The gyration of ions must no longer be neglected. In the extreme case of low $\dot{n}_i$ the stability of an ion ring distribution must be considered. Galeev [10] finds $\eta_e \approx 0.025$ in this limit. This is due to spreading of the ion distribution towards smaller *and* larger velocities, in contrast to the case of an ion beam.

In our experiment, the injection time at maximum range (15 km) was 3 sec. With $\Omega_i(Ba^+) = 30\ s^{-1}$ and $(m_i/m_e)^{1/2} = 500$, $\Omega_i\,\tau_{inj}$ was all the time well below the limit of Equation 20. Hence, the linear beam approximation with its high efficiency, η_e, appears to be appropriate, in agreement with our earlier conclusions.

As to the proposal of Piel and co-workers [5] of an electron current instability (Fig. 6 b), it turns out that very high ionization rates are needed. This can be derived from the velocity threshold for v_D beyond which the modified two-stream instability sets in.

$$v_D > c_s \approx \eta_e^{1/2}\, v_{n\perp}^* \gtrsim v_{crit} \tag{21}$$

would be needed with c_s being the ion-acoustic speed. v_D is related to the momentum balance since the electron drift constitutes the current, j, corresponding to the Lorentz force, i. e.

$$j = -e\,n_i\,v_D = B^{-1}\,m_n\,\dot{n}_i\,v_{n\perp}^*\,. \tag{22}$$

Combining (21) and (22) yields

$$\frac{\dot{n}_i}{n_i\,\Omega_i} > \eta_e^{1/2} \quad \text{or} \quad \Omega_i\,\tau_{inj} \lesssim \eta_e^{1/2}\,. \tag{23}$$

In other words, the deposition time of new ions must be shorter than Ω_i^{-1}. Whereas such short timescales may correctly characterize the formation of density "spokes" in the rotating plasma experiment

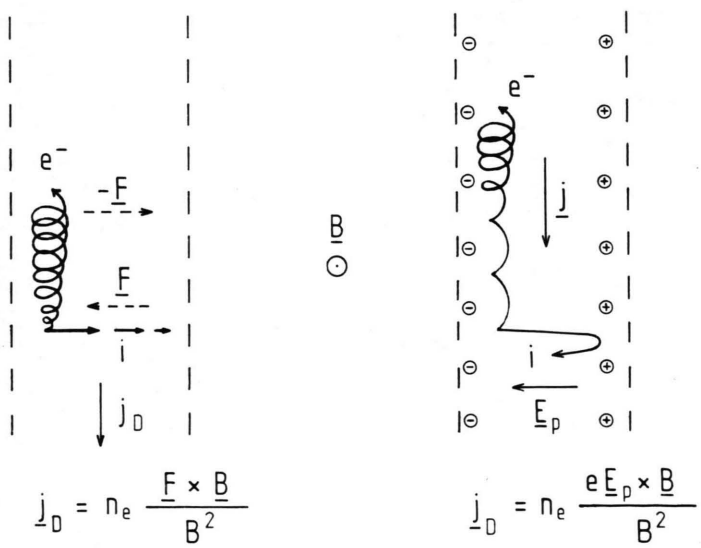

Fig. 6. (left) Ion beam instability slowing down the ions and heating the electrons which perform a mean drift $\boldsymbol{v}_D$. $\boldsymbol{F}$ is the drag force on the ions. (right) A polarization electric field, $\boldsymbol{E}_p$, is set up at a plasma gradient. It decelerates the ions and drives an electron drift, $\boldsymbol{v}_D$ [5].

of Piel and co-workers [5], they do not apply to our experiment. Hence, we are thrown back to the case of a linear ion beam instability.

The lower hybrid waves excited by the ions do not only heat the electrons stochastically by virtue of their small, but finite wave number, $k_{\parallel}$, they also cause a variable transverse drift, v_D. On the average, drift direction and magnitude are consistent with the drag force, $\boldsymbol{F}$, slowing down the ions [27], which must be balanced by the Lorentz force. Hence,

$$\langle \boldsymbol{v}_D \rangle = \frac{\boldsymbol{F} \times \boldsymbol{B}}{e B^2} \,. \tag{24}$$

Part of $\langle \boldsymbol{v}_D \rangle$ may actually be due to a d.c. polarization field, E_p. The two cases of Fig. 6 may be mixed.

It is only the fraction, α_m, of the current in (22) which feeds the shear Alfvén waves considered in the previous section. The rest is confined to the boundary of the hot injected ions and the ambient plasma. This is the diamagnetic current, whose signature was also observed in our experiment.

Summary

The implications of a critical velocity experiment in the upper ionosphere have been discussed. A surprisingly high ionization efficiency was observed ($\approx 30\%$), although the free energy, $\frac{1}{2} m_n v_{n\perp}^{*2}$, was only about four times the ionization potential. This can be understood if the fractional energy transferred to the electrons (tail formation) was rather high ($\eta_e \gtrsim 0.5$). The corresponding momentum is taken up by the magnetic tensions and quickly communicated to the background plasma by emission of a pair of shear Alfvén waves. An extended flux-tube interacts with the injected ions, and the effective mass loading remains small. This explains the rather low electromagnetic perturbations that were observed. The basic instability is identified as that of a linear ion beam constituted by the freshly injected ions. Lower hybrid waves are emitted which slow down the ions and heat the electrons by virtue of their finite parallel wave number.

The discussed experiment (more details will be contained in Paper 2) was the first critical velocity experiment in space allowing a quantitative evaluation of the basic interactions. Another experiment is being planned which will allow us to perform in-situ diagnostics inside the beam. Gas injections from orbiting spacecraft [16] are a good tool to further study this interesting effect which should have many applications in astrophysics [11].

[1] H. Alfvén, On the Origin of the Solar System, Oxford Univ. Press, Oxford 1954.
[2] B. Angerth, L. Block, U. Fahleson, and K. Soop, Nucl. Fus. Suppl. Part I, 39, (1962).
[3] L. Danielsson, Phys. Fluids **13**, 2288 (1970).
[4] G. Himmel, E. Möbius, and A. Piel, Z. Naturforsch. **31a**, 934 (1976).
[5] A. Piel, E. Möbius, and G. Himmel, Astrophysics and Space Science **72**, 211 (1980).
[6] N. Venkataramani and S. K. Mattoo, Pramāna **15**, 117 (1980).
[7] N. Brenning, Experiments on the Critical Velocity Interaction in Weak Magnetic Fields, TRITA-EPP-80-10, Royal Inst. of Technology, Stockholm 1980.
[8] J. C. Sherman, Astrophys. Space Sci. **24**, 487 (1973).
[9] M. A. Raadu, Astrophys. Space Sci. **55**, 125 (1978).
[10] A. A. Galeev, Proc. Internat. School and Workshop on Plasma Astrophysics, Varenna (ESA SP-161), 77 (1981).
[11] E. F. Petelski, in Relation Between Laboratory and Space Plasmas (ed. by H. Kikuchi), D. Reidel Publ. Comp., Dordrecht 1981, p. 23.
[12] L. Danielsson and G. H. Kasai, J. Geophys. Res. **73**, 259 (1968).
[13] V. Formisano, A. Galeev, and R. Z. Sagdeev, The Role of the Critical Ionization Phenomena in the Production of Inner Coma Cometary Plasma, to appear in Planet. Space Sci. (1982).
[14] I. M. Podgorny and Y. V. Andrijanov, Planet. Space Sci. **26**, 99 (1978).
[15] P. A. Cloutier, R. E. Daniell, Jr., A. J. Dessler, and T. W. Hill, Astrophys. Space Sci. **55**, 93 (1978).
[16] E. Möbius, R. W. Boswell, A. Piel, and D. Henry, Geophys. Res. Lett. **6**, 29 (1979).
[17] K. W. Michel, Acta Astronautica **1**, 37 (1974).
[18] E. M. Wescott, H. M. Peek, H. C. Stenbaek-Nielsen, W. B. Murcray, R. J. Jensen, and T. N. Davis, J. Geophys. Res. **77**, 2982 (1972).
[19] G. Haerendel, in Space Research XIII, Akademie Verlag, Berlin 1973, p. 601.
[20] C. S. Deehr, E. M. Wescott, H. Stenbaek-Nielsen, G. J. Romick, T. J. Hallinan, and H. Föppl, A Critical Velocity Interaction Between Fast Barium and Strontium Atoms in the Terrestrial Ionospheric Plasma, Preprint Univ. of Alaska (1981).
[21] H. C. Koons and M. B. Pongratz, J. Geophys. Res. **86**, 1437 (1981).
[22] L. A. Vainshtein, V. I. Ochkur, V. I. Rakhovskii, and A. M. Stepanov, Soviet Physics JETP **34**, 271 (1972).
[23] J. B. McBride, E. Ott, J. P. Boris, and J. H. Orens, Phys. Fluids **15**, 2367 (1972).
[24] L. Danielsson and N. Brenning, Phys. Fluids **18**, 661 (1975).
[25] I. Axnäs, Geophys. Res. Lett. **7**, 933 (1980).
[26] M. Scholer, Planet. Space Sci. **18**, 977 (1970).
[27] M. Lampe and K. Papadopoulos, Astrophys. J. **212**, 886 (1977).